[AMERICAN JOURNAL OF SCIENCE, VOL. 297, SUMMER, 1997, P. 707–728]

GRAIN-SCALE STABLE ISOTOPE DISEQUILIBRIUM DURING FLUID-ROCK INTERACTION. 2: AN EXAMPLE FROM THE PENNINIC-AUSTROALPINE TECTONIC CONTACT IN EASTERN SWITZERLAND

H. EPPEL and R. ABART*

Institut für Mineralogie und Petrographie,
ETH Zentrum, CH-8092 Zürich, Switzerland

ABSTRACT. At the tectonic contact between the Penninic Platta Nappe and the Lower-Austroalpine Err Unit in eastern Switzerland carbon and oxygen isotope fronts are preserved at the interface of serpentinites and low-grade regional metamorphic metacarbonates. The carbon and oxygen isotope compositions of calcite are $\delta^{13}C = 2.3$ permil (PDB) and $\delta^{18}O = 21.0$ permil (SMOW) in the unaltered metacarbonates at a distance of about 20 m from the lithologic contact, and they are $\delta^{13}C = 0.0$ permil and $\delta^{18}O = 14.0$ permil at the metacarbonate-serpentinite interface. The concomitant shift in the oxygen isotope composition of quartz is from 24.0 to 17.0 permil. A peculiarity of the isotope pattern is the systematic variation of the quartz-calcite oxygen isotope fractionations across the isotopic front. Quartz-calcite fractionations are relatively small ($\approx$3.0 permil) in the unaltered metacarbonate and at the metacarbonate-serpentinite interface, and they increase in the transitional zone in between with a maximum of 7.1 permil at a distance of about 2 m from the contact. This pattern is interpreted as a result of advective-dispersive material transport across the lithologic contact and coupled first-order kinetic mineral-fluid exchange. The oxygen isotope systematics indicate that calcite-fluid isotope exchange was fast, and local calcite-fluid equilibrium prevailed during fluid-rock interaction. In contrast, quartz-fluid exchange was relatively sluggish, and the quartz-calcite oxygen isotope fractionations deviated significantly from their equilibrium values. Front geometries suggest that dispersive processes contributed substantially to material transport across the metacarbonate-serpentinite contact. Cross-layer advective flow was minor with a maximum time-integrated volumetric flux of 21 m^3/m^2. From the influence of quartz-fluid exchange kinetics on the intermineral fractionations quantitative relations among transport velocities, the rates of mineral-fluid exchange and the duration of fluid-rock interaction are derived. These relations are then combined with geologic and experimental data to identify "feasible" scenarios of fluid-rock interaction.

INTRODUCTION

The analysis of stable isotope patterns has become a routine method in studies of phenomena of fluid-rock interaction in active and fossil hydrothermal systems. Initially, zero-dimensional box models were used to interpret shifts in isotopic compositions from fluid-rock interaction (Taylor, 1974, 1977). As more detailed information on stable isotope signatures became available, more sophisticated models based on transport theory were em-

* Present address: Institut für Mineralogie-Kristallographie und Petrologie, Karl-Franzens-Universität Graz, Universitätsplatz 2, A-8010 Graz, Austria

ployed (for a review, see Nabelek, 1991; Bickle, 1992; Bowman, Willett, and Cook, 1994).

The formalism provided by transport theory was used by a number of authors to constrain transport processes from the geometry of stable isotope fronts (Ganor, Mathews, and Paldor, 1989; Bickle and Baker, 1990; Jamtveit, Bucher-Nurminen, and Stijfhoorn, 1992; Todd and Evans, 1993; Cartwright, 1994; among others). In these studies, fronts defined by the spatial variation of the isotope compositions of a single monitoring phase or by bulk rock compositions were analyzed. The systematics of inter-mineral isotopic fractionations were not explicitly considered. This makes the distinction between equilibrium and disequilibrium scenarios difficult (Lassey, 1988; Baker and Spiegelman, 1995). This distinction is, however, crucial for the interpretation of stable isotope patterns, because deviations from local equilibrium during fluid-rock interaction may significantly influence front geometries (Lassey and Blattner, 1988; Abart and Sperb, 1997).

Stable isotope compositions of coexisting phases from rocks that underwent fluid-rock interaction have been used in a number of studies to test for the degree of grain-scale isotopic equilibration during fluid-rock interaction (Clayton and Epstein, 1958; Taylor, 1974, 1977; Criss and Taylor, 1986; Gregory and Taylor, 1986; Bickle and others, 1995; among others); for a review of the literature see Gregory, Criss, and Taylor (1989). In these studies explicit information on the system geometry and on the spatial variation of isotope compositions is either missing or is not considered in the analysis. Consequently only limited insight into the processes involved in isotope transport is obtained. Basically, only the distinction between open- and closed-system behavior and an estimation of the degree of external fluid-buffering is possible (Criss, Gregory, and Taylor, 1987).

In several studies more than one isotope tracer was analyzed (Bickle and others, 1988, 1995; Burkhard, Kerrich, and Fyfe, 1992; McCaig and others, 1995; among others). The study of more than one isotope tracer, each with different fluid-solid partitioning, provides a powerful means of understanding the coupling of transport and exchange processes. In particular, pervasive flow and fracture flow can be discriminated (Bickle, 1992).

Although there is a wealth of studies on the isotopic effects of fluid-rock interaction in fossil systems, the number of comprehensive studies that integrate the various types of information, that is the spatial variation of the stable isotope compositions of more than one monitoring phase and in more than one isotope system, in an analysis based on transport theory, is small. Here we present an example of fluid-rock interaction from a tectonic contact in a regional metamorphic terrain in eastern Switzerland. In this case study we integrate data on the spatial variation of isotopic compositions of two monitoring phases and from two isotope tracers. In particular, we make use of the information provided by the systematics of the inter-mineral fractionations to identify deviations from local equilibrium during fluid-rock interaction and to derive quantitative relations among the transport and exchange parameters.

Geologic Setting

Regional geology.–In the Oberhalbstein area (Graubünden, Eastern Switzerland) the boundary between the Penninic and the overlying Austroalpine nappes is located at the Platta Nappe-Err Unit tectonic contact. The geology of the area is described in detail by Cornelius (1950) and Dietrich (1969, 1970). The Platta Nappe is a relict of the former Piemontese-Ligurian Thetys ocean floor, and it is the highest tectonic unit within the Penninic nappe pile (fig. 1). The Platta Nappe is composed of dismembered ophiolitic relics, dominated by metabasalts and serpentinites. Upper Jurassic to Cretaceous metasediments are also present, occurring as disrupted layers and lenses, from several up to a hundred meters thick. The metasediments include a stratigraphic sequence of radiolaria cherts, pelagic limestones, and pelagic limestones interbedded with shales, the so-called Palombini Formation. Overlying the Platta Nappe is the Lower-Austroalpine Err Unit, which is composed of a crystalline basement with a locally preserved Mesozoic sedimentary cover. In some areas the crystalline basement is overlain by the volcanic-sedimentary sequence of the rhyolitic Nair Porphyroid. The Mesozoic sediments have a late Jurassic and Cretaceous facies development similar to the coeval sediments in the Platta Nappe. The Platta Nappe and the Err Unit also underwent similar deformational and metamorphic histories during the Alpine orogeny. The main deformation, D1, took place in the late Cretaceous. It was associated with nappe imbrication of the Austroalpine and the Platta Nappe and produced a penetrative foliation. Later deformation phases were associated with extensional tectonics (D2) and with the northward transport of the Austroalpine Platta Nappe complex (D3) (Froitzheim, Schmid, and Conti, 1994). Deformation during the D2 and D3 events was generally non-penetrative. The main metamorphic overprint in both the Platta Nappe and the Err Unit is ascribed to the late Cretaceous nappe imbrication. It reached lower greenschist facies conditions with peak metamorphic temperatures of 250° to 300°C (Trommsdorff, 1983; Ferreiro Mählmann, 1996). The complex remained at these conditions until the onset of extensional tectonics, and the temperature remained approximately constant during the D1 and D2 deformation events (Liniger, 1992). Nappe imbrication and extensional tectonics have been dated radiometrically by Handy and others (1996). These authors obtained an age of 89 to 76 Ma for the D1 event and 80 to 67 Ma for the D2 event. Carbon and oxygen isotope compositions in the metasediments of the Platta Nappe vary between −2 and 2 permil $\delta^{13}C$(PDB) and 11 to 25 permil $\delta^{18}O$(SMOW). In the metasediment layers of the Platta Nappe, carbon and oxygen isotope ratios are generally depleted toward the lithologic contacts with the surrounding metabasic rocks. This trend is particularly pronounced in a profile across the metacarbonates of the Palombini Formation at the Platta Nappe-Err Unit tectonic contact in the Scalotta region (see fig. 1).

The Palombini Formation in the Scalotta region.–In the Scalotta region the Palombini Formation is about 70 m thick and is sandwiched between serpentinites of the underlying Platta Nappe and the metavolcanics (Nair Porphyroid) of the overlying Err Unit. A schematic lithologic profile of the

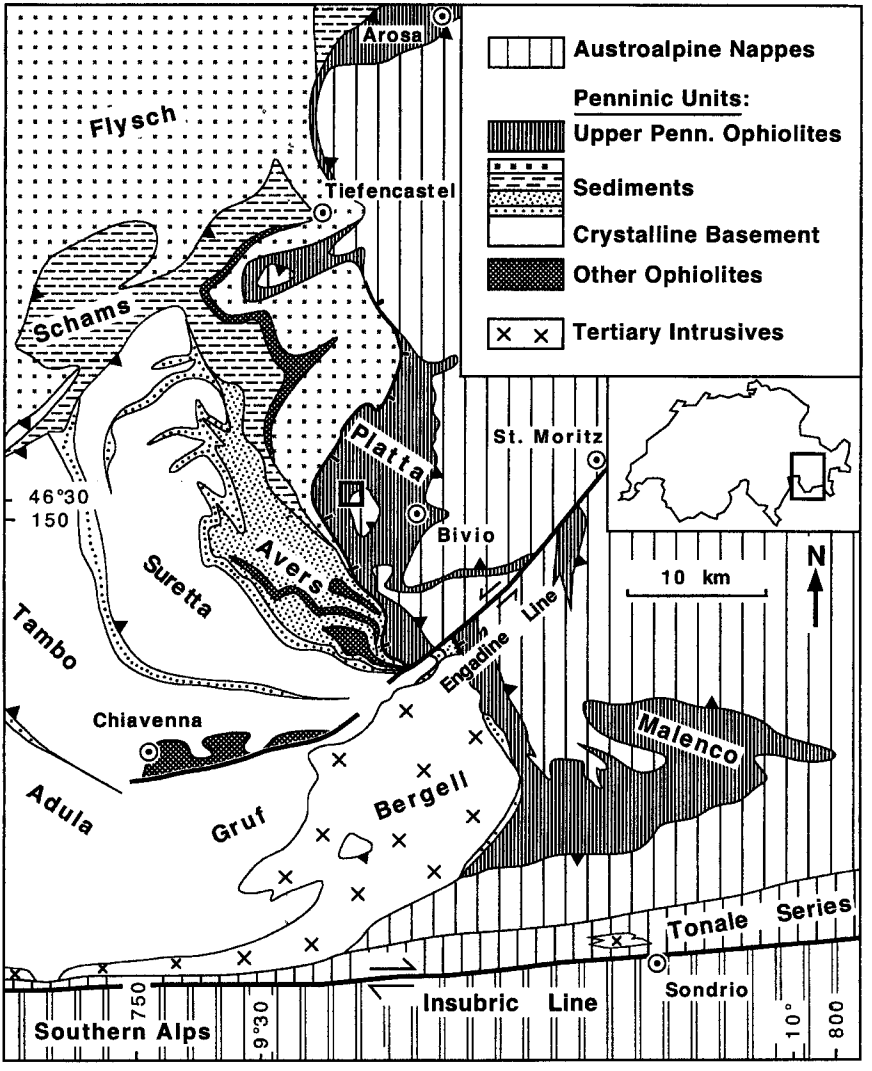

Fig. 1. Geological sketch map of the Penninic-Austroalpine transition in eastern Switzerland–adapted from Nievergelt and others (1996), sampling location in the Scalotta area indicated by small rectangle.

Platta Nappe-Err Unit tectonic contact in the Scalotta region is shown in figure 2. The contacts of the metasediments with the surrounding rocks are tectonic, and they were probably first generated during nappe imbrication (D1). The main foliation produced during D1 is coherent in the metacarbonates and in the underlying serpentinite, indicating that this contact was

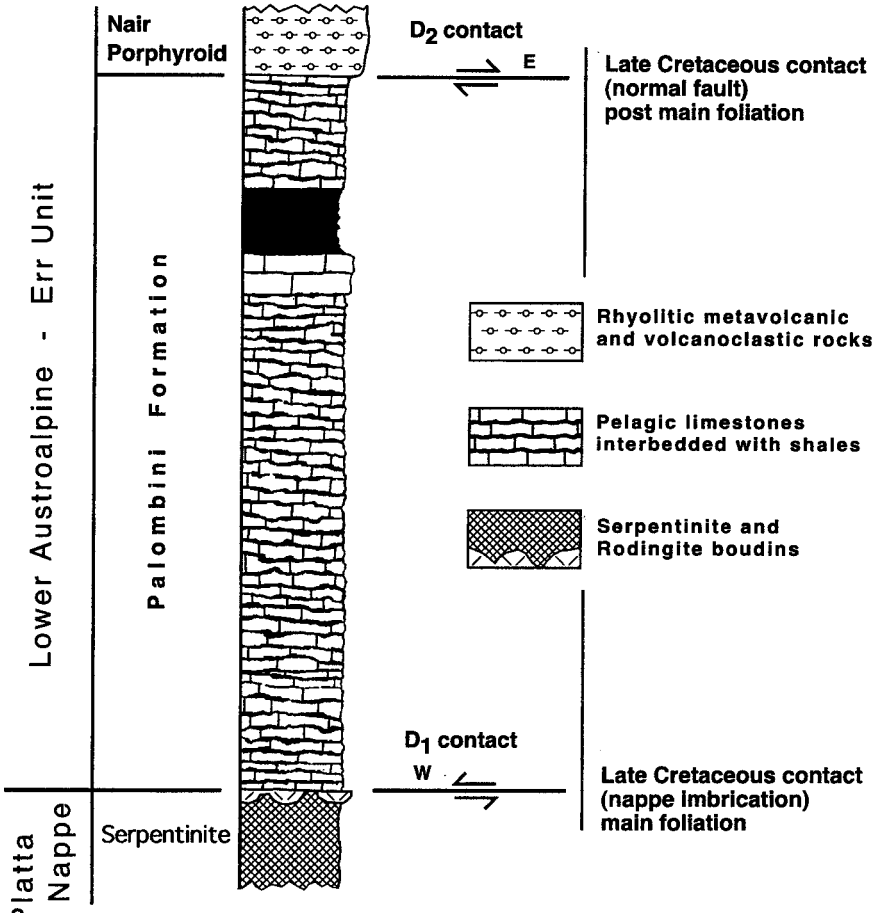

Fig. 2. Schematic lithologic profile across the Palombini Formation at the Platta Nappe-Err Unit tectonic contact; total thickness of the Palombini Formation in the Scalotta region is about 70 m; tectonic contact at the bottom of the section preserved from an early stage of the tectonometamorphic evolution (D_1), tectonic contact at the top of the section reactivated during extensional tectonics (D_2).

preserved in an essentially original state from an early stage of the structural evolution. Strain markers indicate shortening of the metasediment sequence perpendicular to the lithological contact. In a 2.3 m wide contact zone toward the serpentinites, shortening is more intense than in the central zone of the Palombini Formation by a factor of about 5. At the top of the Palombini Formation the main foliation of the metasediments is cut by the tectonic contact with the Nair Porphyroid. This contact was presumably first established during nappe imbrication, and it was probably reactivated during

extensional tectonics and may thus be regarded as a D2 feature. The metasediment section appears to be incomplete at this contact, the top of the section has been truncated during extensional tectonics.

The mineralogical composition of the metasediments is dominated by calcite, which makes up 80 to 90 percent of the rock. Quartz and feldspar comprise another 10 to 15 percent, illite and chlorite are subordinate. With respect to the microtexture, a fine-grained homogeneous matrix and veins with relatively coarse-grained calcite and minor quartz can be distinguished. The bulk of the veins were formed during the D1 event. The veins are up to 1 mm thick, often boudinaged, and they have been rotated into an orientation parallel to the main foliation. In the matrix the grain-size of calcite is generally <20 μm. Quartz grains are usually somewhat larger with grain diameters of about 40 μm. The fabric is characterized by strong preferred orientation of elongate calcite and quartz grains. This fabric was produced during the early penetrative deformation event. The calcite and quartz microtextures indicate crystalloplastic deformation, dynamic recrystallization, and pressure-solution.

Carbon and Oxygen Isotope Systematics

Analytical methods.–The data shown in figure 3 represent samples taken from the homogeneous, fine-grained, quartz- and feldspar-bearing carbonate matrix. Homogeneous rock samples of 20 to 60 g were crushed and sieved.

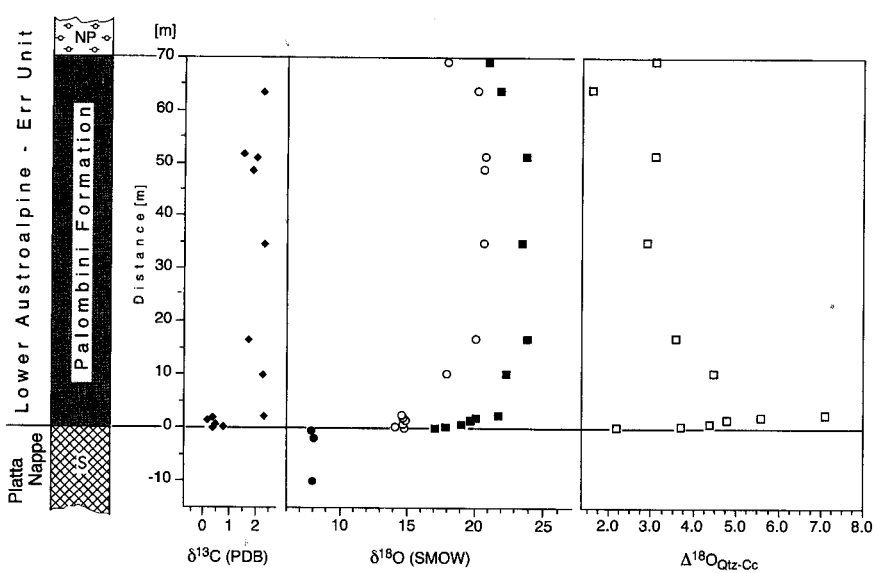

Fig. 3. Carbon and oxygen isotope systematics of the Palombini Formation at the Platta Nappe-Err Unit tectonic contact in the Scalotta area: black diamond symbols–$\delta^{13}C_{calcite}$(PDB), black dots–$\delta^{18}O_{serpentinite}$(SMOW), open circles–$\delta^{18}O_{calcite}$(SMOW), black rectangles–$\delta^{18}O_{quartz}$(SMOW), open rectangles–quartz-calcite oxygen isotope fractionations.

The fraction larger than 125 μm and smaller then 250 μm was split. One subsample was ground to powder and used for conventional CO_2 extraction from carbonates (McCrera, 1950). From the second subsample, carbonate was removed by treatment with acetic acid. Opaque phases and sheet silicates were removed from the residue on a magnetic separator. Inspection of the samples by X-ray diffractometry revealed that all separates contained both quartz and feldspar. In a subsequent step the samples were treated with hydrofluoric acid for 3 min to dissolve feldspar. The samples were then re-examined with X-ray diffractometry. For some samples the HF-treatment had to be prolonged for 30 sec to remove the feldspar quantitatively. The clean quartz separates were then subjected to conventional oxygen extraction by fluorination. For both carbonates and silicates, reproducibility of replicate measurements was better than 0.2 permil in the oxygen system, and it was better than 0.1 permil for carbonates in the carbon system. Carbon and oxygen isotope compositions are given in permil relative to the PDB and SMOW standards.

Stable isotope compositions of calcite and quartz along a profile across the Palombini Formation at the Platta Nappe-Err Unit tectonic contact in the Scalotta area are shown in figure 3. The most striking feature of the stable isotope pattern is the depletion trend toward the lithologic contacts. The profile is somewhat asymmetric. Isotopic depletion in the metasediments is more pronounced at the contact toward the underlying serpentinite than at the contact toward the overlying metavolcanics. The observed asymmetry may be due to differences in the isotopic and hydraulic characteristics of the serpentinites and the Nair Porphyroid. It must, at least in part, be also ascribed to the modifications of the isotope profile during extensional tectonics. The effect of the D2 deformation was to reduce the metasediment sequence at the top of the section. The isotope front is hence incomplete at the contact to the Nair Porphyroid. This is why only the relatively undisturbed contact with the footwall serpentinite will be considered in the following discussion.

Calcite oxygen isotope compositions are successively depleted from $\delta^{13}O = 21.0$ permil in the central portion of the metasediment sequence to 14.0 permil at the lithologic contact. A similar shift from 24.0 to 17.0 permil is observed in coexisting quartz. The oxygen isotope front is relatively smooth and extends over about 20 m into the metasediment layer. Calcite carbon isotope compositions are shifted from $\delta^{13}C = 2.3$ permil in the central portion of the metasediment layer to values between $\delta^{13}C = 0.2$ and 0.8 permil at the lithologic contact. The carbon isotope front is relatively sharp, and it is located at a distance of about 2 m from the lithologic contact. The oxygen isotope fronts monitored by quartz and calcite do not exactly parallel each other, and the quartz-calcite fractionations show a pronounced systematic variation as a function of distance from the lithologic contact. Quartz-calcite fractionations are relatively small, about 3.0 permil, in the central part of the metasediment layer and at the lithologic contact. At intermediate positions the quartz-calcite fractionations increase successively and reach a maximum of 7.1 permil at a distance of 2.5 m from the serpentinite-

metacarbonate interface. The shortening of the metasediment sequence may have modified the original geometry of the stable isotope fronts. This possibility will be considered in the following analysis.

FLUID-ROCK INTERACTION

Prior to fluid-rock interaction the quartz and calcite isotope compositions were most likely constant throughout the metasediment sequence. In the unaltered metacarbonates of the central zone the quartz-calcite oxygen isotope fractionation is about 3.0 permil. According to the calibration of Sharp and Kirschner (1994) this corresponds to a temperature of 265°C. This is in good agreement with temperature estimates from paragenetic information (Trommsdorff, 1983; Ferreiro Mählmann, 1996) and corroborates the view that quartz-calcite local equilibrium prevailed prior to fluid-rock interaction. The trend of ^{18}O depletion of quartz and calcite toward the underlying serpentinite is ascribed to interaction of the metasediments with an externally derived, isotopically light fluid. Fluid-rock interaction most likely occurred during nappe imbrication when the metasediments, the serpentinites, and the Nair Porphyroid were juxtaposed tectonically. The most probable source of ^{18}O depleted oxygen is the volumetrically dominant underlying serpentinites and metabasalts of the ophiolitic Platta Nappe. The metabasic rocks represent a large reservoir of isotopically light oxygen. The bulk rock oxygen isotope composition of the serpentinite is 8.1 permil. Using the serpentinite-water equilibrium fractionation factor for 250°C, $\Delta^{18}O_{Serp\text{-}H_2O} = 1.0$ permil (Wenner and Taylor 1971)[1] a composition of 7.1 permil is calculated for an aqueous serpentinite pore-fluid. The oxygen isotope composition of the serpentinite remains constant up to the serpentinite-metacarbonate contact. This indicates that at the lithologic contact the oxygen isotope composition of the pore fluid was maintained at a constant composition of 7.1 permil in equilibrium with the serpentinite during fluid-rock interaction. The oxygen isotope fronts are contained entirely within the metacarbonates indicating that net oxygen transport was from the serpentinites into the metasediment layer. The processes that may have been involved in material transport across the serpentinite-metacarbonate contact are fluid advection and dispersion[2] in the pore fluid.

Calcite isotope compositions are similar in the early formed calcite veins where grains are up to several millimeters in size and in the matrix carbonate with a grain size generally less than 20 μm. Regardless of the relative timing of vein-formation and fluid-rock interaction, this observation suggests that local calcite-fluid oxygen isotope equilibrium was attained during fluid-rock interaction. The vein-calcites were most probably in isotopic equilibrium with the fluid from which they precipitated. If vein-formation and fluid-rock

[1] The fractionation factor given by Wenner and Taylor (1971) depends on the calibration of the quartz-water oxygen isotope fractionation which has been revised since their publication (Clayton, O'Neil, and Mayeda, 1972; Sharp and Kirschnere, 1994). We use the original expression given by Wenner and Taylor, because, for the temperatures of interest, it is well compatible with the empirical quartz-calcite calibration of Sharp and Kirschner (1994).

[2] In this context the term "dispersion" describes the combined effects of molecular diffusion and hydrodynamic dispersion.

interaction occurred at the same time, then the similarity of the isotopic compositions of vein and matrix calcite suggests that they were both in equilibrium with the local pore fluid. The rates of mineral-fluid isotopic exchange are grain-size sensitive. If the calcite veins already existed at the onset of fluid-rock interaction, the similarity of the isotopic compositions of vein and matrix calcites indicates that both matrix and vein-calcite were shifted to equilibrium with the pore fluid. In either case the independence of calcite isotope compositions from grain size suggests that calcite-fluid exchange was fast relative to material transport and that deviations of the calcite-fluid oxygen isotope fractionations from their equilibrium values during fluid-rock interaction were negligible.

If quartz-calcite local equilibrium had been maintained during fluid-rock interaction, the observed variation in quartz-calcite oxygen isotope fractionations would indicate a pronounced temperature variation across the oxygen isotope front. Based on a local equilibrium assumption relatively high temperatures on the order of 300°C would be inferred from the relatively small quartz-calcite fractionations in the central part of the metasediment layer and at the lithologic contact. Significantly lower temperatures, as low as 80°C, would be obtained from the large quartz-calcite fractionations at intermediate positions. It is improbable that such a temperature variation, of over more than 200°C on a meter-scale, could occur in a regional metamorphic terrain. The systematic variation of the quartz-calcite oxygen isotope fractionations across the isotope front rather suggests that the quartz-calcite fractionations significantly deviated from their equilibrium values during fluid-rock interaction. This disequilibrium feature is readily explained by the interplay of transport and exchange, if both occur at finite rates (Abart and Sperb, 1997). For any given distance from the lithologic contact, the oxygen isotope shift in calcite is larger than the corresponding shift in the coexisting quartz. The oxygen isotope front recorded by quartz lags behind the front recorded by calcite. This indicates that quartz-fluid exchange was slower than oxygen isotope exchange between calcite and the pore fluid. This observation agrees well with literature data on mineral-fluid exchange obtained from both hydrothermal experiments (see Cole and Ohmoto, 1986) and from natural systems (Clayton; Muffler, and White, 1968; Taylor 1974, 1977; among others).

The shifts observed in the metasediment carbon isotope compositions indicate that apart from oxygen also isotopically light carbon-bearing species were introduced into the metasediments. Due to the scarcity of data the carbon isotope front is ill defined, and it cannot be used to extract quantitative information. It does, however, shed light on the coupling of transport and exchange in a qualitative way. The carbon isotope front is significantly retarded with respect to the oxygen isotope front indicating that material transport in a water rich fluid and mineral-fluid isotopic exchange were intimately coupled. This in turn suggests that the fluid pathways were homogeneously distributed on a grain-scale corroborating the use of transport theory to analyse the observational data.

Modeling

Model assumptions.–In our simplified model, the metasediments of the Palombini Formation are treated as an aggregate composed of 90 volume percent calcite and 10 volume percent quartz. Feldspar and sheet silicates are neglected. The bi-mineralic aggregate is regarded as a semi-infinite, one-dimensional system, which extends from the serpentinite-metasediment lithologic contact into the metasediments. The isotopic compositions of quartz, calcite, and the pore fluid are assumed to have been initially constant throughout the metasediments, and it is assumed that all phases were in isotopic exchange equilibrium with one another. The initial compositions of quartz and calcite were taken as the compositions observed in the central part of the metasediment layer, $\delta^{18}O^{init}_{calcite} = 21$ permil and $\delta^{18}O^{init}_{quartz} = 24$ permil, respectively. The initial isotopic composition of the metasediment pore-fluid was calculated as $\delta^{18}O^{init}_{fluid} = 14.3$ permil from the initial composition of calcite and the corresponding equilibrium fractionation factor (O'Neil, Clayton, and Mayeda, 1969). The oxygen isotope composition of the pore fluid at the metacarbonate-serpentinite interface is assumed to have been constant during fluid-rock interaction, and it is assigned a value of $\delta^{18}O^{inf}_{fluid} = 7.1$ permil, in equilibrium with the serpentinite. This corresponds to the "pinned boundary" boundary condition of Bickle and Baker (1990). The processes involved in isotope transport across the lithologic boundary are considered to have been fluid-advection and dispersion in the pore fluid. Calcite-fluid isotopic exchange is considered to have been fast so that local calcite-fluid equilibrium was maintained during fluid-rock interaction. Quartz-fluid oxygen isotope exchange is considered to have occurred at a finite rate. The kinetics of quartz-fluid oxygen isotope exchange are described by a pseudo first-order rate law (Cole, Ohmoto, and Lasaga, 1983). The effective dispersivity, the mean interstitial particle velocity, the rate of quartz-fluid isotopic exchange, the modal mineral abundances, the isotopic composition of the externally derived fluid, and the temperature are considered to have remained constant during fluid-rock interaction.

In the following discussion it will be convenient to express distance from the serpentinite-metacarbonate lithologic contact and isotopic compositions in terms of dimensionless quantities. Dimensionless distance x is obtained by normalizing an actual distance X to an arbitrarily defined scaling length L, $x = X/L$. For the problem at hand the scaling length was chosen to be 10 m. The normalized isotopic composition of a phase k is defined as:

$$R_k = \frac{\delta_k^{obs} - \delta_k^{init}}{\delta_k^{eq} - \delta_k^{init}},$$

where δ_k^{init} is the isotopic composition of phase k before the onset of fluid-rock interaction, δ_k^{eq} is the isotopic composition of phase k in equilibrium with the externally derived fluid, and δ_k^{obs} is the observed isotopic composition of phase k. According to the calcite-water equilibrium fractionation factor given by O'Neil, Clayton, and Mayeda (1969), the oxygen isotope composition of

TABLE 1

Oxygen isotope systematics at the serpentinite-metacarbonate contact

Sample identification	Distance (m) from contact	Dimensionless distance x	Dimensionless distance x′	$\delta^{18}O_{cc}$ (SMOW)	$\delta^{18}O_{qtz}$ (SMOW)	R_{cc}	R_{cc}
Sc4-94-kt	0.02	0.002	0.012	14.9	17.1	0.90	0.98
Sc4-94-1	0.30	0.030	0.144	14.2	17.9	0.97	0.87
Sc4-94-2	0.75	0.075	0.360	14.8	19.1	0.88	0.70
Sc4-94-3	1.35	0.135	0.648	15.0	19.8	0.86	0.59
Sc4-2	1.80	0.180	0.864	14.8	20.2	0.88	0.54
Sc4-94-4	2.30	0.230	1.104	14.7	21.8	0.90	0.30
Sc4-3	10.30	1.030	2.134	18.0	22.5	0.42	0.20
Sc4-4	16.80	1.680	2.784	20.2	23.8	0.10	0.01
Sc4-5	34.80	3.480	4.584	20.8	23.6	0.01	0.04
Sc4-8	48.80	4.880	5.984	20.8	n.a.	0.01	n.a.
Sc4-9	51.31	5.131	6.235	20.9	23.9	0.00	0.00

Actual and normalized oxygen isotope compositions and distances from the serpentinite-metacarbonate contact of samples from the profile across the Palombini Formation in the Scalotta area; scaling distance for the derivation of dimensionless distances is 10 m; column "x"–uncorrected dimensionless distances, column "x′"–dimensionless distances corrected for observed strain in the lowermost 2.3 m of the metasediment section; the last two columns give the isotopic compositions normalized to initial and equilibrium compositions: $\delta^{18}O^{init}_{calcite} = 21‰$, $\delta^{18}O^{init}_{quartz} = 24‰$ $\delta^{18}O^{eq}_{calcite} = 14.0‰$, $\delta^{18}O^{eq}_{quartz} = 17.0‰$.

calcite in equilibrium with the externally derived fluid at about 270°C is 14.0 permil. The corresponding equilibrium composition of quartz is 17.0 permil (Sharp and Kirschner, 1994). The numerical values of the actual and normalized oxygen isotope compositions and distances from the serpentinite-metacarbonate contact are given in table 1. Here we include two sets of dimensionless distances. The column designated "x" is derived from the actual length measurements through scaling with L = 10 m, whereas for the calculation of the dimensionless distances labelled "x′" the length measurements at the bottom 2.3 m of the metasediment sequence were corrected for the observed strain in the contact zone by applying a stretching factor of 4.8. Henceforth the two lists of data triplets "x, R_{cc}, R_{qtz}" and "x′, R_{cc}, R_{qtz}" will be referred to as the "original observational data-set" and the "corrected observational data-set," respectively. Both data sets will be considered in the following analysis to estimate the influence of the strain correction on the transport and exchange parameters obtained from inverse modeling.

Governing equations.–The formalism employed to describe advective-dispersive isotope transport and coupled first-order kinetic mineral-fluid exchange was discussed in detail by Abart and Sperb (1997). For the problem at hand where calcite is in exchange equilibrium with the pore fluid their eq (1) can be rewritten as:

$$D' \frac{\partial^2 R_{cc}}{\partial X^2} - v' \frac{\partial R_{cc}}{\partial X} = \frac{\partial R_{cc}}{\partial t} + \gamma'_{qtz} \frac{\partial R_{qtz}}{\partial t}, \qquad (1)$$

where R_{cc} is the normalized isotopic composition of calcite and the pore fluid,[3] and R_{qtz} is the normalized isotopic composition of quartz, X and t are the space and time coordinates. The parameters D′, the "retarded effective dispersivity," and v′, the "retarded mean interstitial particle velocity," are defined as:

$$D' = \frac{D}{R_t}, \qquad v' = \frac{v}{R_t}$$

where D is the effective dispersivity, and v is the mean interstitial particle velocity, which is related to the Darcy velocity, q, by: $v = q/\phi$, where ϕ is the volumetric porosity. The retardation factor R_t is defined as:

$$R_t = 1 + \frac{\alpha_{cc} X_{cc}}{X_f}.$$

X_i is the fraction of the total oxygen in a control volume contained within phase i; α_i is the mineral i–fluid equilibrium fractionation factor. The parameter γ'_{qtz} in eq (1) is defined as:

$$\gamma'_{qtz} = \frac{X_{qtz}}{X_f + \alpha_{cc} X_{cc}}.$$

The series approximations suggested by Abart and Sperb (1997) then take the form:

$$R_{cc}(y, \tau) = \frac{1}{2} e^{(\sqrt{N_{Pe}}/2)y} G\left(y, \tau \frac{\sqrt{N_{Pe}}}{2}\right) - \epsilon \frac{\beta_{qtz} y e^{(\sqrt{N_{Pe}}/2)y - N^D_{qtz}\tau}}{4\omega_{qtz}} [B(y, \tau, -\omega_{qtz}) - B(y, \tau, \omega_{qtz})] \quad (2)$$

for the normalized isotopic compositions of calcite and the pore fluid and

$$R_{qtz}(y, \tau) = \frac{\alpha_{qtz}}{2} e^{(\sqrt{N_{Pe}}/2)y} \left[G\left(y, \tau, \frac{\sqrt{N_{Pe}}}{2}\right) - e^{-N^D_{qtz}\tau} G(y, \tau, \omega_{qtz}) \right] - \epsilon \left\{ \frac{\alpha_{qtz} N^D_{qtz} y}{2} e^{(\sqrt{N_{Pe}}/2)y} \beta_{qtz} T_{qtz}(y, \tau) \right\} \quad (3)$$

for the normalized isotopic composition of quartz, where

$$y = \sqrt{N_{Pe}}\, x, \qquad \beta_{qtz} = \frac{\gamma_{qtz} \alpha_{qtz} N^D_{qtz}}{\epsilon}, \qquad \omega_{qtz} = \sqrt{\frac{N_{Pe}}{4} - N^D_{qtz}},$$

[3] Given that calcite and the pore fluid are in isotopic exchange equilibrium with each other, their normalized isotopic compositions are identical.

and ϵ is an arbitrarily defined constant <1. The functions $B(y, \tau, s)$, $G(y, \tau, s)$, and $T_k(y, \tau)$ are defined as follows:

$$B(y, \tau, s) = e^{ys}\,\mathrm{erfc}\left(\frac{y}{2\sqrt{\tau}} + s\sqrt{\tau}\right)$$

$$G(y, \tau, s) = B(y, \tau, s) + B(y, \tau, -s)$$

$$T_k(y, \tau) = \frac{1}{\omega_k^2}\left(\frac{\tau}{\pi}\right)^{1/2} Ex\left(y, \tau, \frac{\sqrt{N_{Pe}}}{2}\right) + \frac{1}{4\omega_k^3} e^{-N_k^D \tau}[B(y, \tau, \omega_k)(1 - \omega_k y - 2\omega_k^2\tau) + B(y, \tau, -\omega_k)(-1 - \omega_k y + 2\omega_k^2\tau)]$$

$$Ex(y, \tau, s) = \exp\left[-\left(\frac{y^2}{4\tau} + s^2\tau\right)\right] \qquad (4)$$

Eqs (2) through (4) are written in terms of dimensionless parameters. The Peclet Number N_{Pe} is defined as $N_{Pe} = (v'L)/D'$, the Damköhler Number of quartz, N_{qtz}^D is given by $N_{qtz}^D = (K_{qtz}L)/v'$, where K_{qtz} is the rate of oxygen isotope exchange between quartz and the pore fluid. The corresponding definition of dimensionless time τ is: $\tau = (v't)/L$.

The dimensionless transport and exchange parameters that describe the isotopic effects of fluid-rock interaction in the Palombini Formation, namely the Peclet Number, the Damköhler Number of quartz and dimensionless time, were obtained by minimizing the variance of the observational data with respect to the model prediction. The variance σ^2 is defined as:

$$\sigma^2 = \sum_k \sum_i \frac{(R_k^{obs} - R_k^{mod})^2}{NM}$$

where R_k^{obs} and R_k^{mod} are the observed and modeled, normalized isotopic compositions of phase k at a given position. The sum is over N observations, where each observation includes M mineral phases. The explicit nature of expressions 2 and 3 allows application of efficient optimization procedures, such as the method of steepest descent, to investigate the $N_{Pe} - N_{qtz}^D - \tau$ parameter space.

Results.–For each of the observational data-sets the minimization of σ^2 yields a unique solution for the dimensionless parameters: $N_{Pe} = 0.4$, $N_{qtz}^D = 6.7$, $\tau = 0.2$ are derived from the original observational data-set, $N_{Pe} = 5.5$, $N_{qtz}^D = 1.2$, $\tau = 1.6$ are derived from the corrected observational data-set. Both data sets and the corresponding model outputs are shown in a dimensionless coordinate frame in figure 4. The distribution of the residuals $(R_k^{obs} - R_k^{mod})$ was investigated by means of χ^2 statistics. $\chi^2 = 2.13$ for the original observational data-set, and $\chi^2 = 0.21$ for the corrected observational data-set. χ^2 was calculated for 2 degrees of freedom, and in both cases the χ^2 is

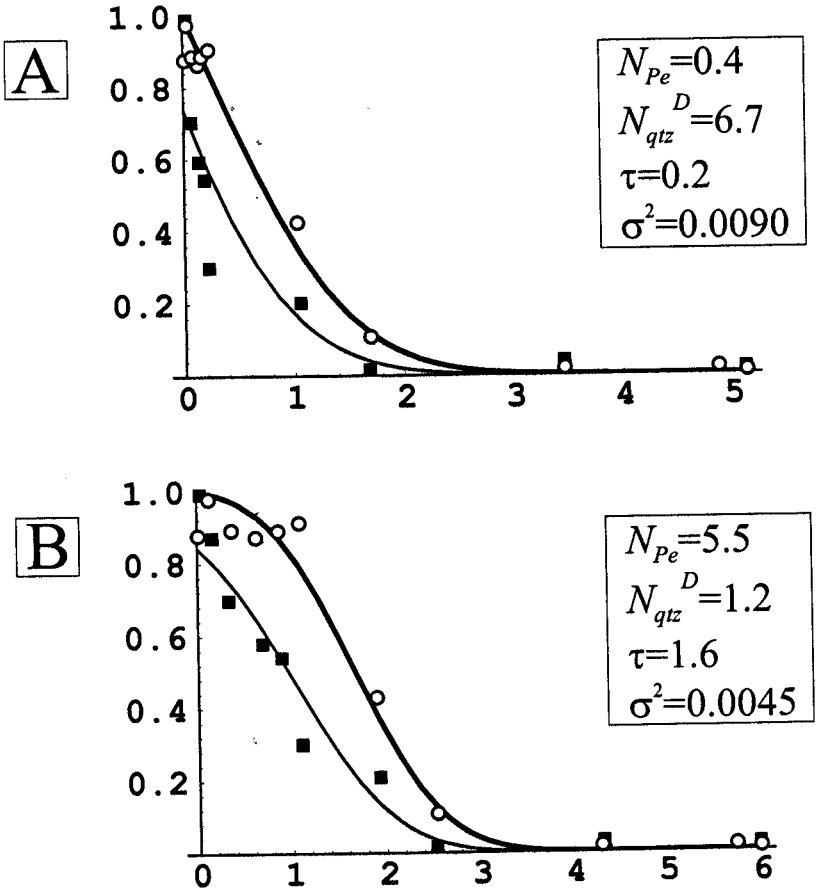

Fig. 4. Comparison of model calculations and observations in a dimensionless coordinate frame, (A) original observational data-set, (B) observational data-set corrected for observed strain in the lowermost 2.3 m of the section; open circles and heavy lines–observed and modeled normalized oxygen isotope compositions of calcite, black squares and thin lines–observed and modeled compositions of quartz.

less then $\chi^2_{2,.10}$, which is 4.61. The residuals may hence be regarded as normally distributed with respect to the predicted mean on a 10 percent level. In this case the variance σ^2, which is also given in figure 4, is an appropriate measure for the quality of fit. The numerical values of the dimensionless parameters depend on the scaling distance, which was chosen arbitrarily. To arrive at a physically meaningful interpretation the dimensionless numbers must be transformed back into the physical parameter space. Upon back-transformation the uniqueness of the solution is lost; the dimensionless numbers yield only quantitative relations among the physical param-

eters. The relations among the retarded effective dispersivity of oxygen, the retarded fluid-particle velocity, the overall rate constant for quartz-fluid oxygen isotope exchange, and the duration of fluid-rock interaction obtained from the original observational data-set may be stated as: $D'/v' = 25$ m, $D'/K_{qtz} = 37.3$ m^2, $D' \cdot t = 50$ m^2. The product $v' \cdot t$ is 2.02 m, that is a "retarded time integrated flux" in the direction perpendicular to the metacarbonate-serpentinite contact. From the corrected observational data-set somewhat different relations are obtained: $D'/v' = 1.8$ m, $D'/K_{qtz} = 15.2$ m^2, $D' \cdot t = 29$ m^2. The corresponding retarded integrated flux is 15.75 m. The above relations may be employed to derive "feasible" sets in the physical parameter space that describe oxygen transport across the serpentinite-metacarbonate contact and coupled mineral-fluid exchange.

DISCUSSION

The correction for the strain observed in the lowermost 2.3 m of the metasediment section has an effect on both the quality of fit and on the dimensionless parameters obtained. The variance is smaller and the fit is better for the corrected observational data-set than for the original data-set. This may indicate that the front geometries were indeed modified by deformation after fluid-rock interaction and that the strain corrected data-set better represents the original geometry of the isotope pattern. The Peclet Number and dimensionless time obtained from the original observational data-set are approximately one order of magnitude smaller than the corresponding parameters obtained from the corrected observational data-set, and the Damköhler Numbers differ by a factor of 5.6. The parameters obtained from the original data-set indicate transport that is more strongly dominated by dispersion and a shorter duration than indicated by the dimensionless parameters obtained from the corrected data-set. Upon back-transformation the differences in dimensionless parameters are propagated into the physical parameter space. Table 2 gives selections of "feasible" parameter sets that could explain the original and the corrected observational data-sets. Independent evidence is required to decide which of these parameter sets best represents the actual process. Note that the parameters D' and v' depend on the retardation factor, R_f, which in turn is a function of the oxygen porosity, X_f. A retarded quantity Ξ' is related to its non-retarded equivalent Ξ by: $\Xi = \Xi'[1 + (\alpha_{cc}X_{CC})/X_f]$. For the problem at hand, where $X_f \ll 1$ and $X_{cc} \approx 1$, this may be approximated by $\Xi \approx \Xi'/X_f$. From the molar volumes of calcite (36.9 cm^{3}mol^{-1}), quartz (22.7 cm^{3}mol^{-1}), and an aqueous fluid at 250°C and 3 to 5 kb ($\approx$16.5 cm^{3}mol^{-1}) a relation between the oxygen porosity, X_f, and the volumetric porosity ϕ can be derived: $X_f \approx 0.75\phi$. This gives the conversion from the "retarded integrated flux" to the integrated volumetric fluid flux. The integrated volumetric fluid flux obtained from the original observational data-set is 2.7 m^3/m^2, and it is 21 m^3/m^2 for the corrected observational data-set.

Geological considerations and experimental data allow some of the physical parameters to be constrained: A maximum estimate for the duration of fluid-rock interaction can be obtained from geochronological data. Fluid-

TABLE 2

Transport- and exchange parameters

$L = 10$ m, $N_{Pe} = 0.4$, $N^{D}_{qtz} = 6.7$, $\tau = 0.2$ $L = 10$ m, $N_{Pe} = 5.5$, $N^{D}_{qtz} = 1.2$, $\tau = 1.6$					
D' m^2s^{-1}	v' ms^{-1}	K_{qtz} s^{-1}	t s	t years	original data-set corrected data-set
$7.9 \cdot 10^{-8}$	$3.2 \cdot 10^{-9}$	$2.1 \cdot 10^{-9}$	$6.3 \cdot 10^{8}$	$2.0 \cdot 10^{1}$	original data-set
$4.6 \cdot 10^{-8}$	$2.5 \cdot 10^{-8}$	$3.1 \cdot 10^{-9}$	$6.3 \cdot 10^{8}$	$2.0 \cdot 10^{1}$	corrected data-set
$7.9 \cdot 10^{-10}$	$3.2 \cdot 10^{-11}$	$2.1 \cdot 10^{-11}$	$6.3 \cdot 10^{10}$	$2.0 \cdot 10^{3}$	original data-set
$4.6 \cdot 10^{-10}$	$2.5 \cdot 10^{-10}$	$3.1 \cdot 10^{-11}$	$6.3 \cdot 10^{10}$	$2.0 \cdot 10^{3}$	corrected data-set
$7.9 \cdot 10^{-12}$	$3.2 \cdot 10^{-13}$	$2.1 \cdot 10^{-13}$	$6.3 \cdot 10^{12}$	$2.0 \cdot 10^{5}$	original data-set
$4.6 \cdot 10^{-12}$	$2.5 \cdot 10^{-12}$	$3.1 \cdot 10^{-13}$	$6.3 \cdot 10^{12}$	$2.0 \cdot 10^{5}$	corrected data-set
$7.9 \cdot 10^{-14}$	$3.2 \cdot 10^{-15}$	$2.1 \cdot 10^{-15}$	$6.3 \cdot 10^{14}$	$2.0 \cdot 10^{7}$	original data-set
$4.6 \cdot 10^{-14}$	$2.5 \cdot 10^{-14}$	$3.1 \cdot 10^{-15}$	$6.3 \cdot 10^{14}$	$2.0 \cdot 10^{7}$	corrected data-set

Sets of physical parameters that describe isotope transport and mineral-fluid exchange in the metasediments of the Palombini Formation. Parameters obtained from both the original observational data-set and the corrected observational data-set are given, see indication in the last column.

rock interaction occurred synchronous to or after nappe imbrication, and it most probably pre-dates the deformation associated with extensional tectonics. According to the findings of Handy and others (1996) this leaves a maximum of 20 my for the duration of fluid-rock interaction. This implies a lower limit on the order of $10^{-14}m^2s^{-1}$ for the retarded effective dispersivity, a lower limit on the order of $10^{-15}ms^{-1}$ for the retarded particle velocity, and a lower limit on the order of $10^{-15}s^{-1}$ for the bulk rate of quartz-fluid oxygen isotope exchange (see table 2).

The dispersion coefficient accounts for the combined effects of molecular diffusion and hydrodynamic dispersion. The effective diffusivity can be roughly estimated from experimental data. The dominant oxygen-bearing species in the pore fluid was H_2O. The diffusivity of the H_2O molecule in free water, D_{H_2O}, is about $4 \cdot 10^{-8}m^2s^{-1}$ at 250° to 300°C and at pressures in excess of 150 MPa (Franck, Wiegand, and Dahmen, 1996). The effective diffusivity of H_2O in a porous rock, D_{eff}, is related to its diffusivity in free water by: $D_{eff} = D_{H_2O} \cdot \phi \cdot \bar{\tau}$, where $\bar{\tau}$ is the tortuosity. In metamorphic rocks the tortuosity may have values between 0.1 and 1.0. The porosity may vary considerably. For the problem at hand it was most probably in the range of 10^{-6} to 10^{-2}. The effective diffusivity of H_2O in the metacarbonates of the Palombini Formation was hence between $4 \cdot 10^{-15}$ and $4 \cdot 10^{-10}m^2s^{-1}$. Considering that $X_f \approx 0.75\phi$, the corresponding retarded effective diffusivities may hence vary between $3 \cdot 10^{-21}m^2s^{-1}$ for porosities of 10^{-6} and a tortuosity of 0.1 and $3 \cdot 10^{-12}m^2s^{-1}$ for porosities of 10^{-2} and a tortuosity of 1; the retarded effective diffusivity would be $4.6 \cdot 10^{-14}m^2s^{-1}$ at a porosity of $3.9 \cdot 10^{-3}$ and a tortuosity of 0.1. For any given porosity and tortuosity, these values must be considered as maximum estimates. They are derived from the relatively fast diffusivity of the H_2O molecule in free water. At low porosities the diffusion of oxygen in a

thin fluid film on mineral surfaces or oxygen diffusion along crystallographic sites at grain boundaries may be significantly slower (Rubie, 1986). Through the geochronological constraints on the maximum duration of fluid-rock interaction the retarded effective dispersivity is limited to values in excess of $4.6 \cdot 10^{-14} m^2 s^{-1}$ (see table 2). Given that fluid-rock interaction lasted for $2 \cdot 10^7$ yrs, the bulk of the effective oxygen dispersivity could be explained by the effect of molecular diffusion, if the porosity were larger than $3.9 \cdot 10^{-3}$. Such a scenario would be compatible with the findings of Cartwright (1994) who ascribed the bulk of dispersivity along and across flow channels in contact metamorphic calc-silicate rocks from the Mary Kathleen fold belt to molecular diffusion. This "maximum-duration scenario" would, however, imply that the rate of quartz-fluid oxygen isotope exchange was very low, on the order of $10^{-15} s^{-1}$ (see table 2). This is several orders of magnitude slower than the corresponding experimentally derived rate constants. Tabulated values of the reaction-specific rate constant for surface-reaction controlled quartz-water oxygen isotope exchange at 250° to 300°C are about 10^{-10} moles $m^{-2} s^{-1}$ (Cole and Ohmoto, 1986). For a quartz grain-size of 40 μm this yields an overall rate constant on the order of $10^{-9} s^{-1}$. If K_{qtz} is assigned a value of $10^{-9} s^{-1}$, this yields a duration of fluid-rock interaction on the order of 10^8s, that is, on the order of years. This "short-time scenario" would imply that the retarded effective dispersivity was on the order of $10^{-8} m^2 s^{-1}$. As the maximum estimate for the retarded effective diffusivity is only $3 \cdot 10^{-12} m^2 s^{-1}$ this would indicate that, in the short-time scenario, the dispersivity of oxygen was almost entirely due to hydrodynamic dispersion, and molecular diffusion contributed only 10^{-2} percent to the bulk dispersivity. The extent of hydrodynamic dispersion depends on flow velocity and on the pore-geometry of the rock. Hydrodynamic dispersion, D_h may be approximated by (Phillips, 1991): $D_h \approx v \cdot l_0$, where l_0 is a "decorrelation distance," which is on the order of the grain size. Considering that $D = 25 \cdot v$ or $D = 1.8 \cdot v$ for the original and the corrected observational data-sets and that the grain size in the metacarbonates is about $2 \cdot 10^{-5}$m, this yields a relative contribution of hydrodynamic dispersion to the bulk dispersivity of $5 \cdot 10^{-2}$ to $3.6 \cdot 10^{-1}$ percent, respectively. Although this relation bears considerable uncertainty, it indicates that the relatively low flow rates across the lithologic contact can not explain the dominance of hydrodynamic dispersion required by the short-time scenario. Alternatively, the contribution of hydrodynamic dispersion may be interpreted as an effect of layer-parallel flow. The layer-parallel component of fluid flow may have been much larger than cross-layer flow,[4] and one may speculate that the associated transversal dispersion has contributed significantly to the effective oxygen dispersivity. A dominance of the contribution from transversal dispersion to the bulk dispersivity would, however, require layer-parallel flow that is at least six orders of magnitude faster than cross-layer flow. For the short-time scenario, this would be on the order of 10^{-3} to $10^{-2} ms^{-1}$. This would require extremely high permeabilities

[4] Bowman, Willet, and Cook (1994) give minimum estimates on the order of $10^3 m^3/m^2$ for the flux along the Glarus thrust, a geological situation which is comparable to the Platta Nappe-Err Unit tectonic contact.

of about 10^{-11} to $10^{-10}m^2$ (see below), which are unlikely to occur in a carbonate rock under metamorphic conditions.

There are no rigorous criteria to constrain the physical parameters within the range given by the two extremal scenarios. Both the maximum-duration scenario and the short-time scenario are controversial. The maximum-duration scenario requires rates of quartz-fluid oxygen isotope exchange several orders of magnitude slower than the corresponding experimentally determined rates; the short-time scenario implies that the bulk of the dispersivity was due to hydrodynamic dispersion, but a dominance of hydrodynamic dispersion is in conflict with the low flow velocities. Several authors (Ganor, Mathews, and Paldor, 1989; Todd and Evans, 1993; Cartwright, 1994; among others) demonstrated that molecular diffusion may contribute significantly to oxygen transport over macroscopically relevant distances. The fact that the estimates regarding the contributions from molecular diffusion to the effective bulk dispersivity become less extreme with decreasing rates of quartz-fluid exchange and increasing duration of fluid-rock interaction leads us to speculate that the rate of quartz-fluid exchange was probably on the order of 10^{-13} to $10^{-11}s^{-1}$. The corresponding maximum contributions of molecular diffusion to the effective dispersivity would then be on the order of a fraction of a percent to several tens of percent. The most probable duration of fluid-rock interaction in accordance with such quartz-fluid exchange rates would be in the range of 10^3 to 10^5 yrs (see table 2).

Based on the assumption that fluid pressure was equal to the lithostatic pressure, minimum estimates for the corresponding intrinsic permeability, k_i, may be derived from the relation:

$$q = \frac{k_i}{\mu} \Delta\rho g,$$

where q is the Darcy velocity, μ is the dynamic viscosity of the fluid, $\Delta\rho$ is the density difference between the rock matrix and the pore fluid, and g is the gravitational acceleration. For the problem at hand we may use values of $\Delta\rho = 1600\ kgm^{-3}$, $\mu_{H_2O} = 1.4 \cdot 10^{-4}$Pas (Walther and Orville, 1982). This yields the relation: $k_i \approx 1.2 \cdot 10^{-8}\ v'$. The intrinsic permeabilities calculated for the "most probable scenario" are thus on the order of 10^{-21} to $10^{-18}m^2$. These values lie well within the range of the permeabilities determined for metamorphic rocks in both laboratory experiments and borehole measurements which vary from 10^{-16} to $10^{-23}m^2$ (Brace, 1980; Clauser, 1991). Our values are also compatible with permeabilities that are considered as typical for metamorphic conditions (Etheridge, Wall, and Vernon, 1983; Thompson and Connolly, 1992; Connolly, 1997; among others).

The preservation of the disequilibrium quartz-calcite oxygen isotope fractionations may shed light on the factors that controlled the duration of fluid-rock interaction. If the rates of isotopic exchange were only controlled by temperature (following an Arrhenius relation), the disequilibrium fractionations should have relaxed during the late stages of regional metamorphism

after fluid-rock interaction had ceased. In such case one would expect the quartz-calcite fractionations either to yield coherent temperatures or to yield closure temperatures that reflect cooling rates (Eiler, Valley, and Baumgartner, 1993). The observed variation of the quartz-calcite fractionations does, however, not correlate with modal mineral abundances, or grain size as would be predicted from the model of the latter authors. The systematic spatial variation of the inter-mineral fractionations may merely be regarded as a consequence of fluid-rock interaction with oxygen transport at finite rates and kinetically controlled mineral-fluid exchange. The preservation of the disequilibrium pattern suggests that oxygen isotope exchange was terminated relatively abruptly and that the isotope pattern remained essentially unchanged after fluid-rock interaction had ceased. This suggests that changes in the deformation regime rather than the thermal evolution during regional metamorphism controlled the duration of fluid-rock interaction.

SUMMARY AND CONCLUSIONS

After the juxtaposition of the Penninic Platta Nappe and the Lower-Austroalpine Err-Unit in the late Cretaceous, carbon and oxygen isotope fronts developed in the metacarbonates of the Palombini Formation at the tectonic contact with the underlying serpentinites. The shapes and relative positions of the carbon and oxygen isotope fronts are compatible with pervasive material transport in a water-rich pore fluid with coupled mineral-fluid exchange. Material transport across the lithologic boundary was due to a combination of fluid advection and dispersion in the pore fluid. Whereas layer-parallel flow may have been substantial, fluid advection across the serpentinite-metacarbonate contact was minor. Dispersive processes contributed significantly to material transport in the direction perpendicular to the lithologic contact. Molecular diffusion may account for the bulk of the dispersive transport only in a "long-time scenario," which is in conflict with experimentally determined rate constants for quartz-water oxygen isotope exchange. A more reasonable scenario with a duration of 10^3 to 10^5 yrs requires that the dispersivity of oxygen was enhanced by the contribution of transversal dispersion associated with layer-parallel flow. The rate of calcite-fluid isotope exchange was fast relative to isotope transport, and calcite-fluid local equilibrium was maintained during fluid-rock interaction. Quartz-fluid exchange was relatively slow, and the quartz-fluid and the quartz-calcite oxygen isotope fractionations significantly deviated from their equilibrium values; a "wave" of quartz-calcite disequilibrium fractionations propagated into the metasediments together with the oxygen isotope front. The preservation of systematic spatial variations in the quartz-calcite fractionations that had developed during fluid-rock interaction suggests that oxygen isotope exchange was terminated relatively abruptly. The duration of fluid-rock interaction was probably controlled by changes in the deformation regime rather than by the thermal evolution of the rocks.

ACKNOWLEDGMENTS

This study was funded through ETH-research fund, grant no. 0-20-014-90. G. Früh-Green, and A.B. Thompson provided valuable advice. We want to thank M. Burkhard, P. Blattner, J.A.D. Connolly, and L. Diamond for fruitful discussions, and we are indebted to B. Jamtveit, A. McCaig, and to an anonymous reviewer for their perceptive and constructive reviews and comments.

REFERENCES

Abart, R., and Sperb, R., 1997, Grain-scale stable isotope disequilibrium during fluid-rock interaction. Part 1: series approximations for advective-dispersive transport and coupled first-order kinetic mineral-fluid exchange: American Journal of Science, v. 297, p. 679–706.

Baker, J., and Spiegelman, M., 1995, Modeling an infiltration-driven geochemical front: Earth and Planetary Science Letters, v. 136, p. 87–96.

Bear, J., 1972, Dynamics of fluids in porous media: New York, Elsevier, 764 p.

Bickle, M., 1992, Transport mechanisms by fluid-flow in metamorphic rocks: oxygen and strontium decoupling in the Trois Seigneurs Massif–a consequence of kinetic dispersion: American Journal of Science, v. 292, p. 289–316.

Bickle, M., and Baker, J., 1990, Advective-diffusive transport of isotopic fronts: an example from Naxos, Greece: Earth and Planetary Science Letters, v. 97, p. 78–93.

Bickle, M., Chapman, H. J., Wickham, S. M., and Peters, M. T., 1995, Strontium and oxygen isotope profiles across marble-silicate contacts, Lizies Basin, East Humbolt Range, Nevada: constraints on metamorphic permeability contrasts and fluid flow: Contributions to Mineralogy and Petrology, v. 121, p. 400–413.

Bickle, M., Wickham, S. M., Chapman, H. J., and Taylor, H. P., Jr., 1988, A strontium, neodymium and oxygen isotope study of hydrothermal metamorphism and crustal anatexis in the Trois Seigneurs massif, Pyrenees, France: Contributions to Mineralogy and Petrology, v. 100, p. 399–417.

Bowman, J. R., Willett, S. D., and Cook, S. J., 1994, Oxygen isotopic transport and exchange during fluid flow: One-dimensional models and applications: American Journal of Science, v. 294, p. 1–55.

Brace, W. F., 1980, Permeability of crystalline and argillaceous rocks: International Journal of Rock Mechanics and Mining Sciences, v. 17, p. 241–251.

Burkhard, M., Kerrich, R., and Fyfe, W. S., 1992, Stable and Sr-isotope evidence for fluid advection during thrusting of the Glarus nappe (Swiss Alps): Contributions to Mineralogy and Petrology, v. 112, p. 293–311.

Cartwright, I., 1994, The two-dimensional pattern of metamorphic fluid flow at Mary Kathleen, Australia: Fluid focussing, transverse dispersion, and implications for modeling fluid flow: American Mineralogist, v. 79, p. 526–535.

Clauser, C., 1991, Permeabilität kristalliner Gesteine. Report No. 107776: Hannover, Germany, Niedersächsisches Landesamt für Bodenforschung.

Clayton, R. N., and Epstein, S., 1958, The relationship between $^{18}O/^{16}O$ ratios in coexisting quartz, calcite and iron oxydes from various geological deposits: Journal of Geology, v. 66, p. 352–372.

Clayton, R. N., Muffler, J. P., and White, D. E., 1968, Oxygen isotope study of calcite and silicates of the River Ranch NO. 1 well, Salton Sea geothermal field, California: American Journal of Science, v. 266, p. 968–979.

Cole, D. R., and Ohmoto, H., 1986, Kinetics of isotope exchange at elevated temperatures and pressures. *in* Valley, J. W., Taylor, H. P., Jr., and O Neil, J. R., editors, Stable isotopes in high temperature geological processes: Reviews in Mineralogy, v. 16, p. 41–90.

Cole, D. R., Ohmoto, H., and Lasaga, A. C., 1983, Isotopic exchange in mineral-fluid systems. I. Theoretical evaluation of oxygen isotopic exchange accompanying surface reactions and diffusion: Geochimica et Cosmochimica Acta, v. 47, p. 1681–1693.

Connolly, J. A. D., 1997, Mid-crustal focussed fluid movement: thermal consequences and silica transport, *in* Jamtveit, B. and Jardly, B. W. D., editors, Fluid flow and transport in rocks, mechanics and effects: London, Chapman & Hall, p. 235–250.

Cornelius, H. P., 1950, Geologie der Err-Julier-Gruppe: Der Gebirgsbau. Beiträge zur geologischen Karte der Schweiz, Neue Folge, v. 70/2, 264 p.

Criss, R. E., Gregory, R. T., and Taylor, H. P., Jr, 1987, Kinetic theory of oxygen isotopic exchange between minerals and water: Geochimica et Cosmochimica Acta, v. 51, p. 1099–1108.

Criss, R. E., and Taylor, H. P., Jr, 1986, Meteoric hydrothermal systems, *in* Valley, J. W., Taylor, H. P., Jr., and O Neil, J. R., editors, Stable isotopes in high temperature geological processes: Reviews in Mineralogy, v. 16, p. 373–424.

Dietrich, V., 1969, Die Ophiolithe des Oberhalbsteins (Graubünden) und das Ophiolithmaterial der ostschweizerischen Molasseablagerungen, ein petrographischer Vergleich: Europäische Hochschulschriften. Reihe XVII, Erdwissenschaften, v. 1, (H Lang & Cic., Bern.)

——— 1970, Die Stratigraphie der Platta Decke: Eclogae Geologicae Helvetiae, v. 63/2, p. 631–771.

Eiler, J. M., Valley, J. W., and Baumgartner, L. P., 1993, A new look at stable isotope thermometry: Geochimica et Cosmochimica Acta, v. 57, p. 2574–2583.

Etheridge, W. A., Wall, V. J., and Vernon, R. H., 1983, High fluid pressures during regional metamorphism and deformation: Journal of Geophysical Research, v. 89 (B12), p. 4344–4358.

Ferreiro-Mählmann, R., 1996, Das Diagenese Metamorphose Muster von Vitrinitreflexion und Illit-"Kristallinität" in Mittelbünden und Oberhalbstein. Teil 2: Korrelation kohlenpetrographischer und mineralogischer Parameter: Schweizerische Mineralogische und Petrographische Mitteilungen, v. 76, p. 23–46.

Franck, E. U., Wiegand, G., and Dahmen, N., 1996, Water, *in* Ullmann's Encyclopedia of Industrial Chemistry, v. 28A, p. 12, Weinheim, Verlag Chemie.

Froitzheim, N., Schmid, S. M., and Conti, P., 1994, Repeated change from crustal shortening to orogenparallel extension in the Austroalpine units of Graubünden: Eclogae Geologicae Helvetiae, v. 87, p. 559–612.

Ganor, J., Mathews, A., and Paldor, N., 1989, Constraints on effective diffusivity during oxygen isotope exchange at a marble-schist contact. Sifnos (Cyclades), Greece: Earth and Planetary Science Letters, v. 94, p. 208–216.

Gregory, R. T., Criss, R. E., and Taylor, H. P. Jr., 1989, Oxygen isotope exchange kinetics of mineral pairs in closed and open systems: applications to problems of hydrothermal alteration of igneous rocks and precambrian iron formations: Chemical Geology, v. 75, p. 1–42.

Gregory, R. T., and Taylor, H. P. Jr., 1986, Possible non-equilibrium oxygen isotope effects in mantle nodules: an alternative to the Kyser-O'Neil-Carmichael $^{18}O/^{16}O$ geothermometer: Contributions to Mineralogy and Petrology, v. 93, p. 114–119.

Handy, M. R., Herwegh, M., Kamber, B. S., Tietz, R., and Villa, I., 1996, Geochronologic, petrologic and kinematic constraints on the evolution of the Err-Platta boundary, part of a fossil continent-ocean suture in the Alps (eastern Switzerland): Schweizerische Mineralogische und Petrographische Mitteilungen, v. 76, p. 453–474.

Jamtveit, B., Bucher-Nurminen, K., and Stijfhoorn, D. E., 1992, Contact metamorphism of layered shale-carbonate sequences in the Oslo rift: I Buffering infiltration and the mechanisms of mass transport: Journal of Petrology, v. 33, p. 377–422.

Lassey, K. R., 1988, Stable isotope fronts and crustal buffering–1-dimensional mass balance and kinetics, *in* Bridgewater D., editor, Fluid movements . . . and the composition of the crust: Proceedings of the NATO workshop Bergen 1987, Reidel NATO Series, p. 1–11.

Lassey, K. R., and Blattner, P., 1988, Kinetically controlled oxygen isotope exchange between fluid and rock in one-dimensional advective flow: Geochimica et Cosmochimica Acta, v. 52, p. 2169–2175.

Liniger, M., 1992, Der ostalpin-penninische Grenzbereich im Bereich der nördlichen Margna Decke (Graubünden, Schweiz): Diss ETH, Nr. 9769.

McCaig, A. M., Vayne, D. M., Marshall, J. D., Banks, D., and Henderson, J., 1995, Isotopic and fluid inclusion studies of fluid movement along the Gavarnie thrust, Central Pyrenees: Reaction fronts in carbonate mylonites: American Journal of Science v. 295, p. 309–343.

McCrea, J. M., 1950, On the isotope chemistry of carbonates a paleotemperature scale: Journal of chemical Physics, v. 18, p. 849–857.

Nabeleck, P. L., 1991, Stable isotope monitors, *in* Kerrick, D. M., editor, Contact metamorphism: Reviews in Mineralogy, v. 26, p. 395–435.

Nievergelt, P., Liniger, M., Froitzheim, N., und Ferreiro Mählmann, R., 1996, Early to mid-Tertiary crustal extension in the Central Alps: The Turba Mylonit Zone (Eastern Switzerland): Tectonics, v. 15, p. 329–340.

O'Neil, J. R., Clayton, R. N., and Mayeda, T. K., 1969, Oxygen isotope fractionations in divalent metal carbonates: Journal of chemical Physics, v. 51, p. 5547–5558.

Phillips, O. M., 1991, Flow and reactions in permeable rocks. Cambridge, Cambridge University Press, 285 p.

Rubie, D. C., 1986, The catalysis of mineral reactions by water and restrictions on the presence of aqueous fluid during metamorphism: Mineralogical Magazine, v. 50, p. 399–415.

Sharp, Z. D., and Kirschner, D. L., 1994, Quartz-calcite oxygen isotope thermometry: A calibration based on natural isotopic variations: Geochimica et Cosmochimica Acta, v. 58, p. 4491–4501.

Taylor, H. P., Jr., 1974, The application of oxygen and hydrogen isotope studies to problems of hydrothermal alteration and ore deposition: Economic Geology, v. 69, p. 843–883.

—— 1977, Water/rock interaction and the origin of H_2O in granitic batholiths: Journal of the Geological Society of London, v. 133, p. 509–558.

Thompson, A. B., and Connolly, J. A. D., 1992, Migration of metamorphic fluid: some aspects of mass and heat transfer: Earth Science Reviews, v. 32, p. 107–132.

Todd, C. S., and Evans, B. W., 1993, Limited fluid-rock interaction at marble-gneiss contacts during Cretaceous granulite-facies metamorphism, Seward Peninsula, Alaska: Contributions to Mineralogy and Petrology, v. 114, p. 27–41.

Trommsdorff, V., 1983, Metamorphose magnesiumreicher Gesteine: Kritischer Vergleich von Natur, Experiment und thermodynamischer Datenbasis: Fortschritte der Mineralogie, v. 61, p. 283–308.

Walther, J. V., and Orville, P. M., 1983, Volatile production and transport in regional metamorphism: Contributions to Mineralogy and Petrology, v. 79, p. 252–257.

Wenner, D. B., and Taylor, H. P., 1971, Oxygen and hydrogen isotope studies of the serpentinization of ultramafic rocks in oceanic environments and continental ophiolite complexes: American Journal of Science v. 273, p. 207–239.